Relationship between threading dislocation and leakage current in 4H-SiC diodes

Hirokazu Fujiwara,[1,a)] Hideki Naruoka,[1] Masaki Konishi,[1] Kimimori Hamada,[1] Takashi Katsuno,[2] Tsuyoshi Ishikawa,[2] Yukihiko Watanabe,[2] and Takeshi Endo[3]
[1]*Toyota Motor Corporation, Toyota, Aichi 470-0309, Japan*
[2]*Power Electronics Research Division, Toyota Central R&D Laboratories Inc., Nagakute, Aichi 480-1192, Japan*
[3]*Research Laboratories, DENSO CORPORATION, Nisshin, Aichi 470-0111, Japan*

(Received 2 March 2012; accepted 1 May 2012; published online 11 June 2012)

The impact of threading dislocation density on the leakage current of reverse current-voltage (I–V) characteristics in Schottky barrier diodes (SBDs), junction barrier Schottky diodes, and p-n junction diodes (PNDs) was investigated. The leakage current density and threading dislocation density have different positive correlations in each type of diode. Consequently, the correlation in SBDs is strong but weak in PNDs. Nano-scale inverted cone pits were observed at the Schottky junction interface, and it was found that leakage current increases in these diodes due to the concentration of electric fields at the peaks of the pits. The threading dislocations were found to be in the same location as the current leakage points in the SBDs but not in the PNDs. © *2012 American Institute of Physics*. [http://dx.doi.org/10.1063/1.4718527]

Recent requirements for power devices for electric vehicles, hybrid vehicles, fuel cell vehicles, and power conversion include the capability to handle larger currents and an increased active area. However, commercial silicon carbide (SiC) diodes only have a rated current of between 6 and 50 A, and a small size of 1.0–12 mm^2.[1,2] In contrast, SiC diodes used in hybrid systems have a rated current of several hundred A and an active size of at least 25 mm^2.[3] However, as the active size increases, product yield deteriorates dramatically due to greater leakage current in reverse current-voltage (I–V) characteristics and decreasing breakdown voltage.[4] It is widely known that several types of crystal defects in epitaxial wafers cause reverse I–V characteristics to deteriorate.[5–10] The risk of these crystal defects occurring increases in accordance with the size of the active area, resulting in lower product yield. Although the impact of threading dislocations on device characteristics has been studied, there has been little agreement on the relationship between I-V characteristics and threading dislocation density.[4,11–16] In addition, there are also different types of threading dislocations. These include screw dislocations, edge dislocations, and basal plane dislocations. The impact of each type of dislocation on leakage current and breakdown voltage has been studied in p-n junction diodes (PNDs).[17–19] And these papers have identified the correlation by which threading dislocations cause leakage current to increase. As described in the previous report, a positive correlation has been identified between leakage current density and threading dislocation density in junction barrier Schottky diodes (JBSDs) in very small leakage current regions when the diode is reverse-biased.[4] Additionally, the surface morphologies of leakage current sources of Schottky barrier diode (SBD) were analyzed using atomic force microscopy (AFM). Nano-sized circular cone shaped pits were observed at the leakage current sources.[15] However, the impact of threading dislocations on leakage current has not been identified for each of the different types of diodes such as SBD, JBSD, and PND. The purpose of this study was to examine the impact of threading dislocation density on leakage current in SBD, JBSD, and PND and to identify the mechanism that threading dislocations cause diode leakage current to increase.

Three types of SiC diodes were fabricated. Figure 1 illustrates the vertical sectional structure of these three types of diodes. The diodes were fabricated on a 4H-SiC (0001), 3-in. N-type wafer. The thickness of the drift layer was 13 μm, and the donor concentration was 5×10^{15} cm^{-3}. Molybdenum (Mo) and Nickel (Ni) contacts were used for the anode and cathode electrode, respectively. After forming each contact by vapor deposition, post-annealing processes were performed for the Mo contact at 800 °C and for the Ni contact at 1050 °C. P^+ regions with an acceptor concentration of 1×10^{19} cm^{-3} were formed in the JBSD and PND at a depth of 700 nm by aluminum (Al) ion implantation. In the same way, Al ion implantation was used to form the field limiting ring at the edge termination structures. Diodes with different areas (active areas: 12.0, 0.79, 0.28, and 0.13 mm^2) were located within a chip size of 6×6 mm^2, and a total of 53 SBD, JBSD, and PND chips were fabricated.

The relationship between the leakage current density in reverse I–V characteristics and the threading dislocation density was investigated as follows. First, the reverse I–V characteristics were evaluated at room temperature. Next, after removing the partial cathode electrode, the leakage points on application of a reverse voltage of −1200 V were analyzed by emission microscopy (Hamamatsu Photonics PHEMOS-1000). The leakage points were marked to an accuracy of ±2 μm using a focused ion beam (FIB). Then, after removing the anode electrode using H_2SO_4/H_2O_2, the surface morphology of the leakage points was measured using AFM (Veeco Nanoscope V). Finally, the threading dislocation

[a)]Electronic mail: fujiwara@hirokazu.tec.toyota.co.jp. Tel.: +81-565-46-3397. Fax: +81-561-46-3382.

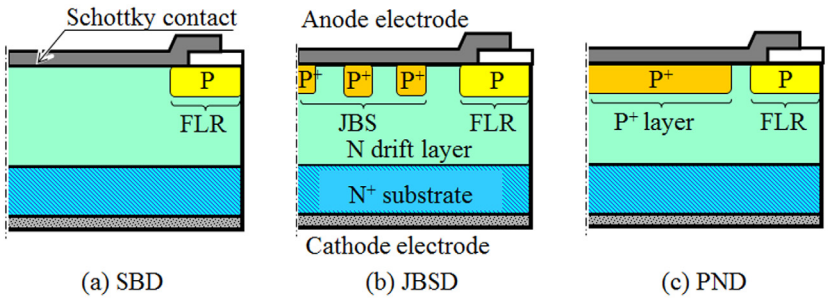

FIG. 1. Sectional structure of diodes: (a) SBD, (b) JBSD, and (c) PND.

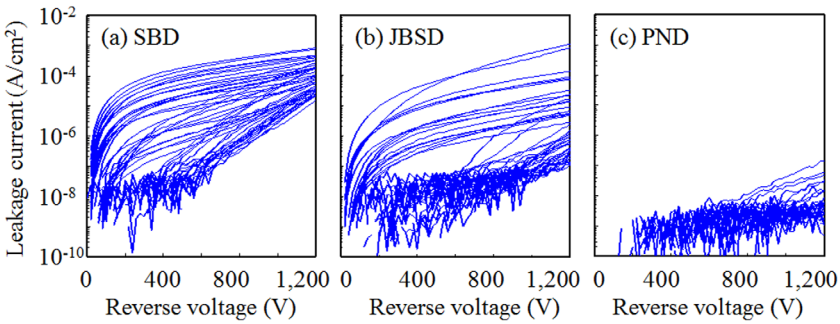

FIG. 2. Reverse I–V characteristics of diodes: (a) SBD, (b) JBSD, and (c) PND.

density was evaluated by a laser microscope after defect-selective etching using a potassium hydroxide (KOH) alkaline solution at 500 °C for 5 min.

Figure 2 shows the reverse I–V waveform in the SBDs, JBSDs, and PNDs (12.0 and 0.79 mm^2). The SBD leakage current varied from 2×10^{-8} A/cm^2 to 2×10^{-4} A/cm^2 at 600 V and from 2×10^{-5} A/cm^2 to 8×10^{-4} A/cm at −1200 V. The JBSD leakage current variation was even larger, ranging from 3×10^{-9} A/cm^2 to 9×10^{-5} A/cm^2 at −600 V and from 1×10^{-7} A/cm^2 to 1×10^{-3} A/cm^2 at −1200 V. In contrast, the PND leakage current was only 1×10^{-7} A/cm^2 or less and 7×10^{-9} A/cm^2 or less for most diodes. Diodes with no surface abnormalities such as surface crystal defects within the active area, a normal ideal factor, and breakdown voltage were selected from the fabricated diodes. These were used to investigate the relationship between the leakage current density and the threading dislocation density. Figure 3 shows this relationship in SBDs, JBSDs, and PNDs with an applied voltage of −1200 V. The area ratio between the Schottky junction and p-n junction regions was 10:3 in JBSD1 and 5:3 in JBSD2. In the SBDs, when the threading dislocation density increased from 1600/cm^2 to 12700/cm^2, the leakage current increased from 1×10^{-5} A/cm^2 to 1×10^{-4} A/cm^2. Pearson's product-moment correlation coefficient was 0.77, which indicates a close correlation. In the JBSDs, when the threading dislocation density increased from 1200/cm^2 to 12800/cm^2, the leakage current increased from 6×10^{-8} A/cm^2 to 1×10^{-6} A/cm^2. The JBSD correlation coefficient was 0.44, which indicates a fairly close correlation. Although no significant difference was found between JBSD1 and JBSD2, the leakage current in JBSD2 showed virtually no increase when the threading dislocation density exceeded 5000/cm^2. In the PNDs, the leakage current remained virtually unchanged in accordance with the increasing threading dislocation density. The correlation coefficient was only 0.34, which indicates a weak correlation. Therefore, the impact of threading dislocations on leakage current differs for each diode, and each diode has a different correlation between leakage current density and threading dislocation density.

In addition, several diodes were analyzed by emission microscopy to identify the leakage points with an applied voltage of −1200 V. The leakage points and the locations of the threading dislocations were then compared. Figure 4 shows images of the emission points (i.e., the leakage points) and laser microscope images after KOH etching that show the locations of the threading dislocations in the SBDs, JBSDs, and PNDs. In the SBDs, 15 emission points and 14 threading dislocations were observed. Of these dislocations, 13 were in the same location as the emission points, a proportion of 93%. In the JBSDs, 6 emission points and 31 threading dislocations were identified. Of these, 4 were in the same location as the emission points, a proportion of 13%. In the PNDs, 1 emission point and 22 threading dislocations were identified, but the locations did not match. In other words, the probability of alignment between threading dislocations and leakage points grew as the proportion of the

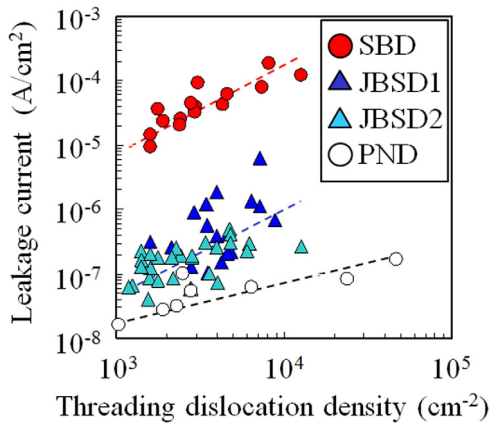

FIG. 3. Relationship between leakage current density and threading dislocation density.

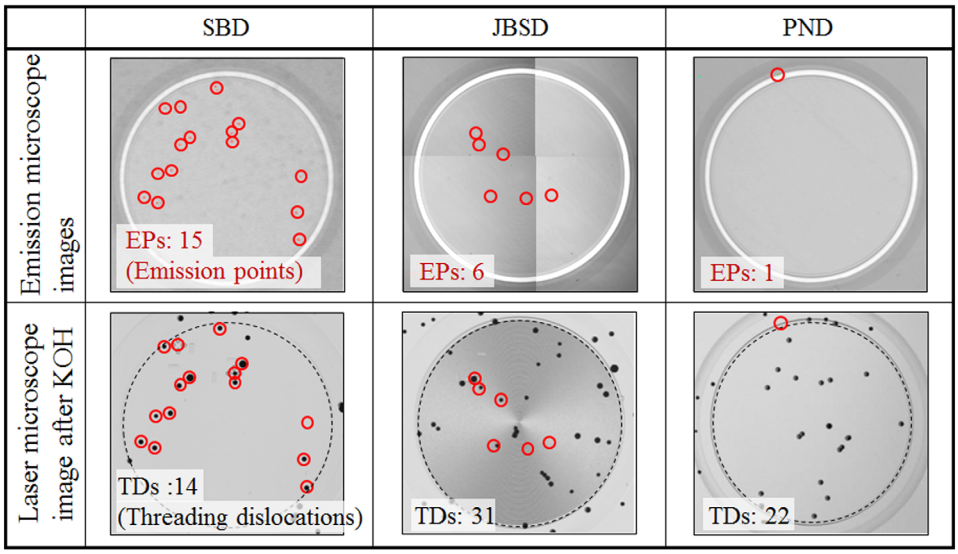

FIG. 4. Emission microscope images at −1200 V and laser microscope images after KOH etching.

area of the Schottky junction region increased. Consequently, the structure of the leakage points in the SBDs was investigated in more detail. After marking the emission points using FIB and removing the surface Mo contact, the SiC surface morphology of the emission points was measured by AFM. Inverted cone-shaped nano-scale pits with a diameter of approximately 200 nm, a depth of approximately 45 nm, and a peak angle of 135° were found at the emission points.[15] Figure 5 shows a sectional transmission electron microscope (TEM) image of a nano-scale pit. In the image, the nano-scale pit is located directly above a threading dislocation that penetrates the SiC drift layer, in other words, on the Schottky junction interface. Accordingly, the nano-scale pits have a major impact on leakage current in SBDs. However, it was assumed that nano-scale pits with a depth of 45 nm and threading dislocations have virtually no impact on PNDs since the p-n junction interface is located 700 nm from the surface in these diodes. In addition, JBSDs have smaller electric field concentrations at the pit ends than in SBDs because the Schottky junction area is smaller than in SBDs and because the junction barrier Schottky (JBS) structure alleviates the electric field at the Schottky junction interface when the diode is reverse biased. However, results clearly show that the impact of a different correlation between different types of threading dislocations and the leakage current was not obtained in this case. Moreover, the same breakdown voltage of diodes with either edge dislocation or screw dislocation was obtained. The reason to be estimated was the effect of nano-scale pit was larger than the effect of own dislocation crystalline defect, and many threading dislocations including edge dislocation and screw dislocation were present in the relatively large active area in these diodes. Further detailed investigation into the generating mechanism of nano-scale pit is required on the device process.

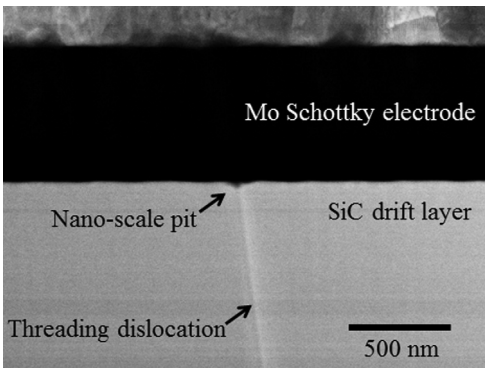

FIG. 5. Sectional TEM image of nano-scale pit directly above threading dislocation.

In summary, this study investigated the relationship between the nano-scale pits located directly above threading dislocations and the leakage current of reverse I–V characteristics in SBDs, JBSDs, and PNDs. The leakage current density and threading dislocation density have different positive correlations in each type of diode. The correlation coefficients of SBD, JBSD, and PND were 0.77, 0.44, and 0.34, respectively. The nano-scale pits with a depth of approximately 45 nm located directly above threading dislocations were found at these leakage points. In SBDs, the source of the leakages at the Schottky junction interface was the nano-scale pits and threading dislocations, 93% of which were located within the active area. However, in the p-n junction regions of JBSDs and PNDs, nano-scale pits and threading dislocations have virtually no impact on the generation or increase in leakage current because the p-n junction interface is located 700 nm from the surface which is deeper than the nano-scale pits.

The authors would like to thank T. Ohnishi and A. Adachi of Toyota Motor Corporation and T. Morino and T. Yamamoto of Denso Corporation for helpful discussions. The authors also would like to thank M. Iida and A. Mikami of Toyota Motor Corporation for the measurements of emission microscopy.

[1]P. Friedrichs, in 2010 International Power Electronics Conference (IPEC), Sapporo, Japan, 21–24 June 2010, p. 3241.
[2]M. K. Das, J. J. Sumakeris, B. A. Hull, J. Richmond, S. Krishnaswami, and A. R. Powell, Mater. Sci. Forum **483–485**, 965 (2005).
[3]T. Yamamoto, J. Kojima, T. Endo, E. Okuno, T. Sakakibara, and S. Onda, Mater. Sci. Forum **600–603**, 939 (2008).
[4]H. Fujiwara, M. Konishi, T. Ohnishi, T. Nakamura, K. Hamada, T. Katsuno, Y. Watanabe, T. Endo, T. Yamamoto, K. Tsuruta, and S. Onda, Mater. Sci. Forum **679–680**, 694 (2011).

[5]T. Kimoto, N. Miyamoto, and H. Matsunami, IEEE Trans. Electron Devices **46**(3), 471 (1999).
[6]P. G. Neudeck, Mater. Sci. Forum **338–342**, 1161 (2000).
[7]D. T. Morisette and J. A. Cooper, Mater. Sci. Forum **389–393**, 1133 (2002).
[8]R. A. Berechman, M. Skowronski, and Q. Zhang, J. Appl. Phys. **105**, 074513 (2009).
[9]H. Fujiwara, T. Kimoto, T. Tojo, and H. Matsunami, Appl. Phys. Lett. **87**, 051912 (2005).
[10]T. Katsuno, Y. Watanabe, H. Fujiwara, M. Konishi, T. Yamamoto, and T. Endo, Jpn. J. Appl. Phys., Part 1 **50**, 04DP04 (2011).
[11]Q. Wahab, A. Ellison, C. Hallin, A. Henry, J. Di Persio, R. Martinez, and E. Janzén, Mater. Sci. Forum **338–342**, 1175 (2000).
[12]H. Saitoh, T. Kimoto, and H. Matsunami, Mater. Sci. Forum **457–460**, 997 (2004).
[13]T. Tsuji, T. Tawara, R. Tanuma, Y. Yonezawa, N. Iwamuro, K. Kosaka, H. Yurimoto, S. Kobayashi, H. Matsuhata, K. Fukuda, H. Okumura, and K. Arai, Mater. Sci. Forum **645–648**, 913 (2010).
[14]B. A. Hull, J. J. Sumakeris, M. J. O'Loughlin, J. Zhang, J. Richmond, A. R. Powell, M. J. Paisley, V. F. Tsvetkov, A. Hefner, and A. Rivera, Mater. Sci. Forum **600–603**, 931 (2008).
[15]T. Katsuno, Y. Watanabe, H. Fujiwara, M. Konishi, H. Naruoka, J. Morimoto, T. Morino, and T. Endo, Appl. Phys. Lett. **98**, 222111 (2011).
[16]A. Grekov, Q. Zhang, H. Fatima, A. Agarwal, and T. Sudarshan, Microelectron. Reliab. **48**, 1664 (2008).
[17]P. G. Neudeck, W. Huang, and M. Dudley, Solid State Electron. **42**, 2157 (1998).
[18]R. A. Berechman, M. Skowronski, S. Soloviev, and P. Sandvik, J. Appl. Phys. **107**, 114504 (2010).
[19]F. Zhao, M. M. Islam, B. K. Daas, and T. S. Sudarshan, Mater. Lett. **64**, 281 (2010).